Destabilization of ERBB2 Transcripts by Targeting 3′ Untranslated Region Messenger RNA Associated HuR and Histone Deacetylase-6

Gary K. Scott,[1] Corina Marx,[1] Crystal E. Berger,[1] Laura R. Saunders,[2] Eric Verdin,[2] Stefan Schäfer,[3] Manfred Jung,[3] and Christopher C. Benz[1]

[1]Buck Institute for Age Research, Novato, California; [2]Gladstone Institute of Virology and Immunology, University of California, San Francisco, California; and [3]Institute of Pharmaceutical Sciences, University of Freiburg, Freiburg, Germany

Abstract

In addition to repressing *ERBB2* promoter function, histone deacetylase (HDAC) inhibitors induce the accelerated decay of mature ERBB2 transcripts; the mechanism mediating this transcript destabilization is unknown but depends on the 3′ untranslated region (UTR) of ERBB2 mRNA. Using ERBB2-overexpressing human breast cancer cells (SKBR3), the mRNA stability factor HuR was shown to support ERBB2 transcript integrity, bind and endogenously associate with a conserved U-rich element within the ERBB2 transcript 3′ UTR, coimmunoprecipitate with RNA-associated HDAC activity, and colocalize with HDAC6. HDAC6 also coimmunoprecipitates with HuR in an RNA-dependent manner and within 6 hours of exposure to a pan-HDAC inhibitor dose, that does not significantly alter cytosolic HuR levels or HuR binding to ERBB2 mRNA. Cellular ERBB2 transcript levels decline while remaining physically associated with HDAC6. Knockdown of HDAC6 protein by small interfering RNA partially suppressed the ERBB2 transcript decay induced by either pan-HDAC or HDAC6-selective enzymatic inhibitors. Three novel hydroxamates, ST71, ST17, and ST80 were synthesized and shown to inhibit HDAC6 with 14-fold to 31-fold greater selectivity over their binding and inhibition of HDAC1. Unlike more potent pan-HDAC inhibitors, these HDAC6-selective inhibitors produced dose-dependent growth arrest of ERBB2-overexpressing breast cancer cells by accelerating the decay of mature ERBB2 mRNA without repressing *ERBB2* promoter function. In sum, these findings point to the therapeutic potential of HuR and HDAC6-selective inhibitors, contrasting ERBB2 stability effects induced by HDAC6 enzymatic inhibition and HDAC6 protein knockdown, and show that ERBB2 transcript stability mechanisms include exploitable targets for the development of novel anticancer therapies. (Mol Cancer Res 2008;6(7):1250–8)

Introduction

Although the overexpressed receptor tyrosine kinase encoded by the amplified *ERBB2* oncogene is a well-validated therapeutic target, there remains a clinical need for newer anti-ERBB2 therapeutic strategies. Following a high-throughput screen of cell-permeable drug-like small molecules, nonspecific histone deacetylase (HDAC) inhibitors emerged as a promising drug class capable of selectively repressing endogenous *ERBB2* promoter function; curiously, such pan-HDAC inhibitors were subsequently found capable of rapidly destabilizing mature ERBB2 transcripts (1-3). The antitumor and anti-ERBB2 properties of pan-HDAC inhibiting hydroxamates such as trichostatin A (TSA), vorinostat (suberoylanilide hydroxamic acid/SAHA; Merck & Co.), and LAQ824 (Novartis Pharmaceuticals) were validated against different ERBB2-overexpressing breast cancer cell lines (e.g., SKBR3, BT474, MDA-453), a trastuzumab-sensitive ERBB2-positive breast cancer xenograft model (e.g., BT474), and a trastuzumab-resistant ERBB2-positive breast cancer xenograft model (B585); in all these studies, tumor growth inhibition correlated with selective down-regulation of ERBB2 transcript and protein levels (1-4).

We initially explored how pan-HDAC inhibitors capable of repressing *ERBB2* gene transcription might also accelerate the decay of mature cytoplasmic ERBB2 transcripts. An ERBB2-independent breast cancer cell line (MCF7) was transfected by paired luciferase expressing constructs, one with and one without downstream insertion of the *ERBB2* 3′ untranslated region (UTR), which contains an evolutionarily conserved U-rich regulatory element putatively capable of binding transcript stability factors such as HuR or AUF1 (refs. 5, 6; Fig. 1A). After either transient or stable introduction of the reporter genes, cells treated with a pan-HDAC inhibitor (TSA, 5-10 hours) showed substantially reduced mRNA and protein expression of the ERBB2 3′ UTR-regulated reporter, suggesting that endogenous ERBB2 transcripts might be similarly regulated (7). To date, neither AUF1 nor HuR have been shown to bind the ERBB2 3′ UTR, although high cytoplasmic levels of the shuttling factor, HuR, have recently been associated with poorer prognosis breast cancers (8).

Received 10/22/07; revised 3/25/08; accepted 3/27/08.
Grant support: NIH sponsored grants R01-CA36773 and P50-CA58207 (UCSF Breast Specialized Programs of Research Excellence), and Hazel P. Munroe memorial funding (Buck Institute). The Hans and Gertie Fischer-Foundation and a Sanofi-Aventis [i]-travel award (S. Schäfer and M. Jung).
The costs of publication of this article were defrayed in part by the payment of page charges. This article must therefore be hereby marked *advertisement* in accordance with 18 U.S.C. Section 1734 solely to indicate this fact.
Requests for reprints: Gary K. Scott, Buck Institute for Age Research, 8001 Redwood Boulevard, Novato, CA 94945. Phone: 415-209-2286; Fax: 415-209-2232. E-mail: gscott@buckinstitute.org

doi:10.1158/1541-7786.MCR-07-2110

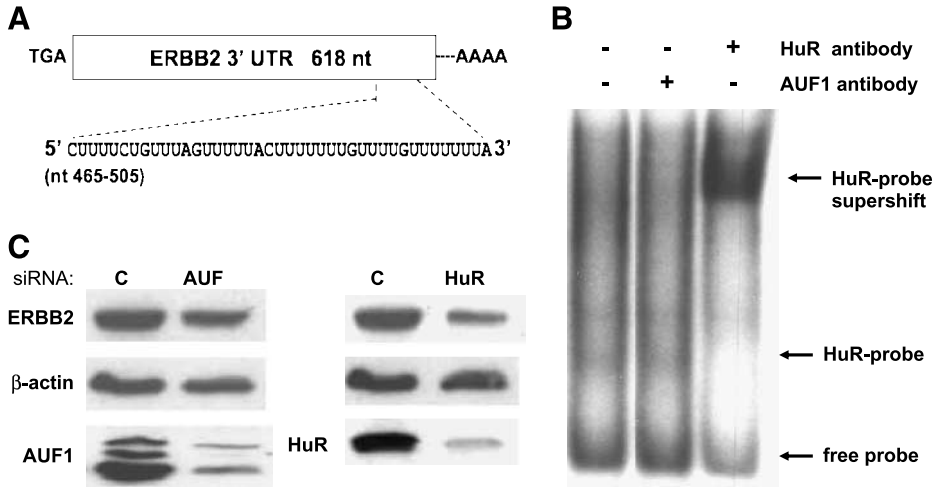

FIGURE 1. ERBB2 expression is regulated by the transcript stability factor, HuR, which binds a conserved U-rich element in the 3′ UTR of ERBB2 mRNA. **A.** Near the poly(A) tail of the ERBB2 3′ UTR is an evolutionarily conserved U-rich region (nucleotides 465-505). **B.** *In vitro* binding assay using SKBR3 cytosol showing that HuR, but not AUF1, is capable of binding to a radiolabeled probe consisting of the conserved U-rich element of the ERBB2 3′ UTR mRNA. The HuR antibody induces a supershift in the HuR-probe complex with loss of the higher mobility probe-bound HuR band. **C.** Immunoblots showing down-regulation of cytosolic AUF1 and HuR levels after siRNA treatment (48 h) of SKBR3 cells, with resultant effects on ERBB2 levels normalized to β-actin.

Cytosolic 3′ UTR binding proteins such as AUF1 and HuR, or other regulators of mRNA translation and stability, have not previously been identified as HDAC substrates. In some cell systems, pan-HDAC inhibitors have been shown to significantly reduce cytosolic (but not total) HuR levels by acetylation of importin-α1, resulting in the reduced stability of HuR target transcripts (9). Unlike HuR, HDAC6 is known to be primarily cytoplasmic in locations in which it functions to deacetylate such substrates as the chaperoning protein HSP90, the microtubule component α-tubulin, and the actin cytoskeleton protein cortactin (3, 10-13). The unique protein structure of HDAC6, with its tandem catalytic deacetylase domains and carboxy terminal binding-of-ubiquitin zinc finger domain (BUZ) found almost exclusively in deubiquitinating enzymes, also suggests that HDAC6 serves largely nongenomic cell functions (13). In fact, HDAC6 has been shown to play essential microtubule, cytoskeleton, and dynein motor–associated roles in regulating cell migration, macropinocytosis, protein trafficking, and accumulation of misfolded proteins into the aggresome (10-13). Some of these nongenomic functions may not require HDAC6 catalytic activity, yet all seem to be dependent on the noncatalytic BUZ (13, 14). Although HDAC6 is generally acknowledged to be extranuclear in both its location and function, nuclear translocation of HDAC6 by chromatin-associated proteins has also been described (12, 13). A recent immunohistochemical study of normal and malignant breast tissues has also noted that HDAC6 is localized primarily in the nucleus of normal mammary epithelial cells but largely in the cytoplasm of most breast cancer cells (15). Thus, although HDAC6 is a logical HDAC candidate to be involved in the maintenance of ERBB2 cytoplasmic mRNA stability in human breast cancer cells, to date, there have been no reports identifying any specific HDAC with eukaryotic regulation of mRNA translation or stability.

The present study was undertaken to further investigate HDAC regulation of ERBB2 transcript stability in an ERBB2-positive human breast cancer cell line, SKBR3. We observed that ERBB2 transcript levels are dependent on cytosolic HuR, which binds to the evolutionarily conserved U-rich region in the 3′ UTR of ERBB2 mRNA, coprecipitates with HDAC enzymatic activity, and colocalizes with cytosolic HDAC6. In turn, HDAC6 immunoprecipitates are enriched with HuR. A series of novel HDAC6-selective inhibitors were synthesized and shown to produce antiproliferative effects at culture concentrations that failed to repress nuclear *ERBB2* promoter activity but induced the decay of mature ERBB2 mRNA and reduced ERBB2 protein levels. In contrast to the ERBB2-inhibiting effects of catalytic pan-HDAC and HDAC6-selective inhibitors, knockdown of HDAC6 protein in SKBR3 by small interfering RNA (siRNA) produced a paradoxical increase in ERBB2 protein expression with no effect on transcript levels, demonstrating that HDAC6 enzymatic inhibition and protein down-regulation are not functionally equivalent. HDAC6 knockdown, however, offset ERBB2 mRNA decay induced by either pan-HDAC or HDAC6-selective inhibitors.

Results

As shown in Fig. 1A, embedded near the poly(A) tail of the *ERBB2* 3′ UTR sequence is an evolutionarily conserved U-rich region (nucleotides 465-505) putatively capable of binding factors such as HuR or AUF1 that regulate mRNA stability (5, 6). Although both AUF1 and HuR are abundantly expressed in SKBR3 cells, Fig. 1B shows that only HuR is capable of *in vitro* binding to the conserved terminal U-rich element (nucleotides 465-505) of the ERBB2 3′ UTR mRNA. Treatment of SKBR3 cells with a pan-HDAC inhibitor (TSA, 0.4 μmol/L ×20 hours) capable of destabilizing ERBB2 mRNA neither induced AUF1 nor inhibited HuR binding to this ERBB2 3′ UTR probe (data not shown). Consistent with the *in vitro* observation of HuR binding to ERBB2 mRNA, siRNA-mediated down-regulation of AUF and HuR protein levels in SKBR3 cells showed that after 48 hours, only HuR down-regulation was associated with altered intracellular expression of ERBB2 (Fig. 1C).

HuR immunoprecipitated from SKBR3 cells showed endogenous binding to ERBB2 transcripts and associated RNA-dependent HDAC activity. As shown in Fig. 2A, immunoprecipitated HuR contained specifically increased levels of ERBB2 mRNA, detected by reverse transcription-PCR using ERBB2-specific primers chosen to amplify a 137-nucleotide sequence

within the ERBB2 3′ UTR just upstream of the conserved U-rich region (nucleotides 465-505). In contrast, control immunoprecipitates from SKBR3 contained almost undetectable levels of ERBB2 mRNA, and both control and HuR immunoprecipitates showed comparable levels of nonspecifically associated glyceraldehyde-3-phosphate dehydrogenase (GAPDH) mRNA. Using a commercial fluorogenic deacetylation assay to monitor total HDAC enzymatic activity, these same ERBB2 mRNA-associated HuR immunoprecipitates were found to contain 3-fold higher HDAC activity than control immunoprecipitates, and this increased HDAC activity was shown to be dependent on HuR-associated mRNA because it was eliminated by concomitant RNase treatment (Fig. 2B). Because the majority of cytosolic HDAC activity is thought to be due to HDAC6, SKBR3 cytosols were subjected to immunoprecipitation-immunoblotting to detect any physical association between HuR and HDAC6. As shown in Fig. 2C, HuR immunoprecipitates were enriched in HDAC6 and HDAC6 immunoprecipitates were enriched in HuR. Interestingly, pretreatment of SKBR3 for 3 hours with a pan-HDAC inhibitor (0.4 μmol/L TSA) did not significantly alter these immunoprecipitation-immunoblot results; however, RNase pretreatment of the SKBR3 cytosols abolished the coassociation of HuR with HDAC6 (data not shown). Microscopic imaging studies were undertaken to further address the apparent physical association between HuR and HDAC6. As seen in Fig. 2D, confocal immunofluorescence imaging confirmed the major nuclear and minor cytoplasmic abundance of HuR (green image) and the major cytoplasmic and minor nuclear abundance of HDAC6 (red image) in normally growing SKBR3 cells. Planar merging of these digitized confocal images readily showed the nuclear and cytoplasmic colocalization of HuR with HDAC6 (yellow image).

Functional relationships between ERBB2, HuR, and HDAC6 in SKBR3 cells were explored using catalytic inhibitors of pan-HDAC enzymatic activity (HDACi: TSA or LAQ824) and

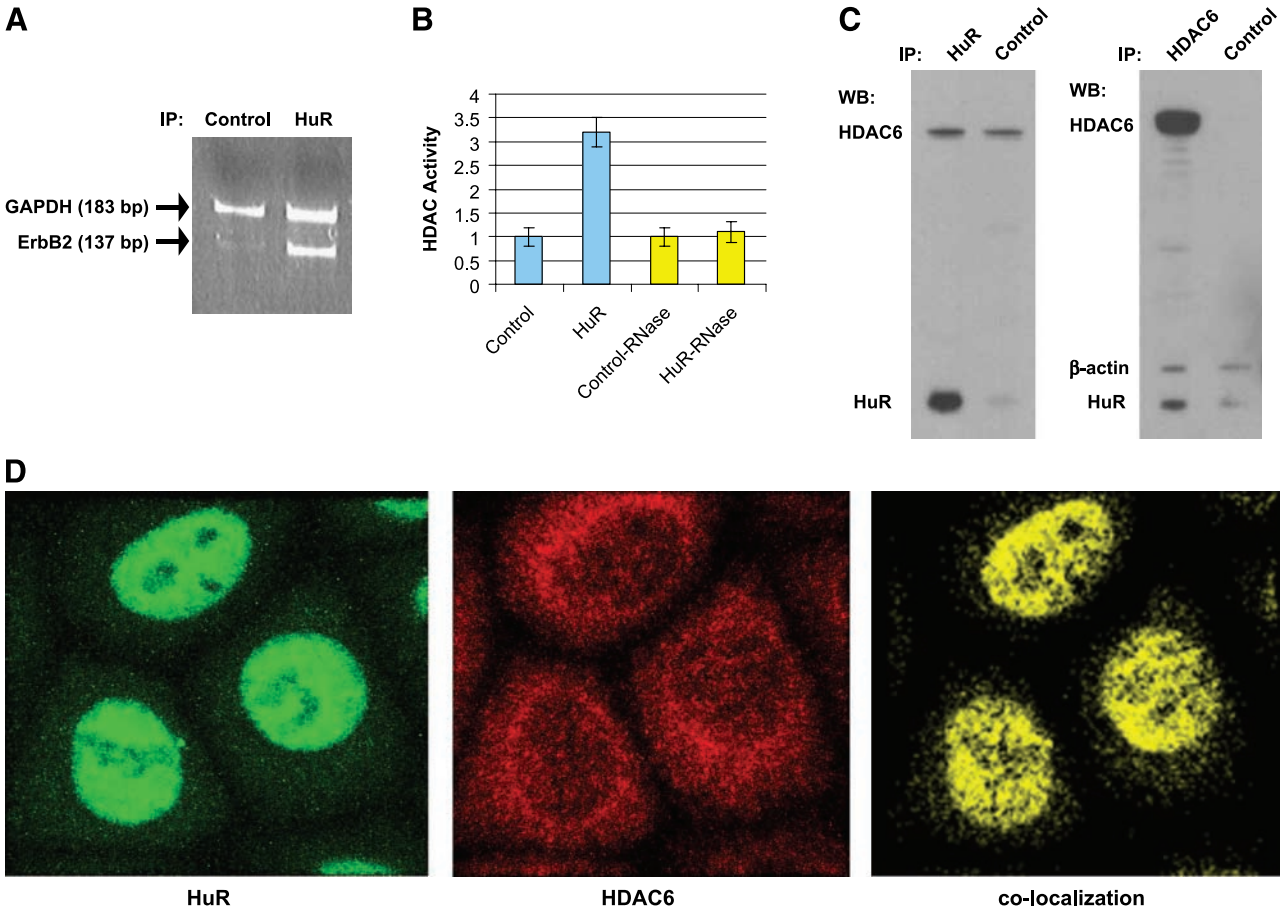

FIGURE 2. Association of cytosolic HuR with ERBB2 mRNA and HDAC enzymatic activity and the coprecipitation and colocalization of HuR with HDAC6 in SKBR3 cells. **A.** Immunoprecipitation of cytoplasmic HuR by specific (or isotype control) antibody followed by reverse transcription-PCR assessment of coprecipitated ERBB2 and GAPDH transcripts. PCR primer pairs were chosen to amplify a 137-nucleotide sequence within the ERBB2 3′ UTR or a 183-nucleotide sequence within GAPDH transcripts. **B.** Following control or HuR immunoprecipitations from SKBR3 cytosols ± RNase treatment, a fluorogenic deacetylation assay was used to monitor coprecipitating total HDAC enzymatic activity. **C.** SKBR3 cytosolic lysates subjected to immunoprecipitation (*IP*) followed by Western blotting (*WB*), demonstrating HuR immunoprecipitation enriched with HDAC6 and HDAC6 immunoprecipitation enriched with HuR (also compared with β-actin coprecipitation). Longer WB exposures (data not shown) confirmed equivalent lane loading by IgG heavy and light chain band intensities. **D.** Immunofluorescence microscopic imaging (40× objective with 4× digital zoom) showing major nuclear and minor cytoplasmic abundance of HuR (*green*) and major cytoplasmic and minor nuclear abundance of HDAC6 (*red*) and their nuclear and cytoplasmic colocalization (*yellow*) in cultured SKBR3 cells.

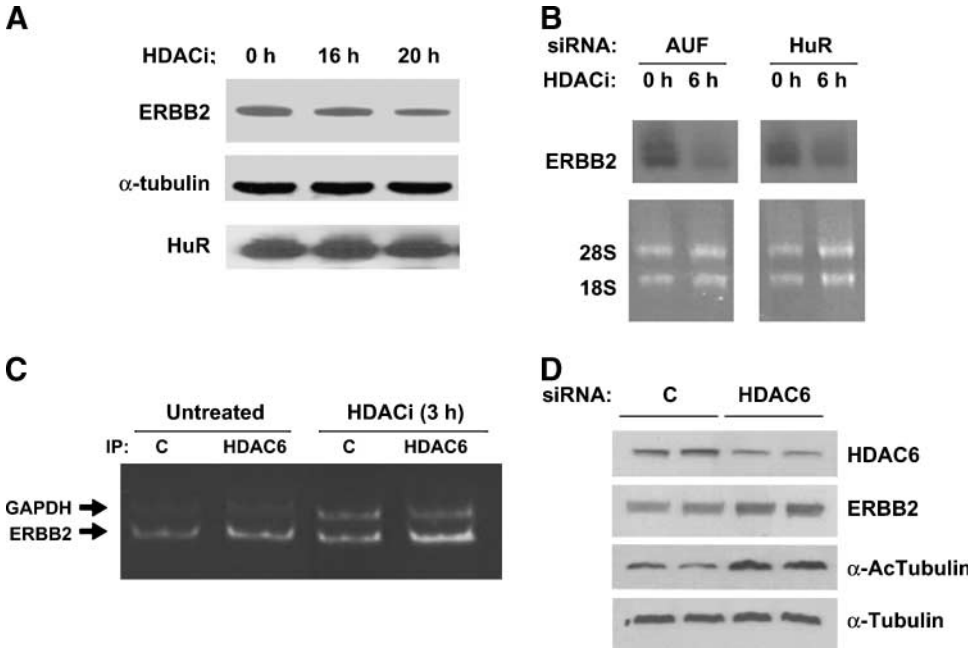

FIGURE 3. ERBB2 effects of pan-HDAC enzymatic inhibitors (*HDACi*) are independent of HuR levels and associated with transcript binding to HDAC6, but dissimilar to that of HDAC6 protein down-regulation by siRNA. **A.** ERBB2 protein inhibition after 16 to 20 h of SKBR3 treatment with TSA (0.4 μmol/L), with no effect on total HuR expression. **B.** Effect of AUF1 or HuR down-regulation by siRNA treatment (48 h, as described in Fig. 1) followed by 6 h of treatment with LAQ824 (10 μmol/L) on SKBR3 ERBB2 mRNA levels (normalized to 28S and 18S rRNA). **C.** Immunoprecipitation of cytoplasmic HDAC6 followed by reverse transcription-PCR assessment of coprecipitated ERBB2 and GAPDH transcripts (as described in Fig. 2) from control cells (*Untreated*) and SKBR3 cells treated with LAQ824 (*HDACi*) for 3 h. Untreated and HDACi reverse transcription samples were PCR-amplified for 24 and 26 cycles, respectively. **D.** HDAC6 knockdown by siRNA (72 h) in SKBR3 cells and resultant effects on ERBB2 and acetylated α-tubulin levels, normalized to total α-tubulin.

siRNA induced down-regulation of HuR (or AUF1) and HDAC6 protein levels. As shown in Fig. 3A, even after 20 hours of SKBR3 treatment with TSA (0.4 μmol/L), the cellular levels of HuR remained unchanged whereas ERBB2 protein levels showed the expected level of decline as previously reported (1). Although total HuR levels remained unchanged, 3 to 6 hours of TSA treatment produced <30% reduction in SKBR3 cytosolic HuR levels (data not shown), a much less pronounced reduction in cytosolic HuR levels as reported in other TSA-treated cell systems (9). To determine how much the destabilization of ERBB2 transcripts by HDACi depended on intracellular HuR or AUF1, 48 hours of siRNA pretreatment was used to first reduce HuR or AUF1 levels and cells were then treated with LAQ824 (10 μmol/L ×6 hours) or drug vehicle. As shown in the Northern blots of Fig. 3B, pan-HDAC inhibition substantially reduced ERBB2 mRNA levels following AUF1 down-regulation and had a slightly attenuated ERBB2 mRNA reducing effect following HuR down-regulation. Note that in the absence of HDACi, HuR down-regulation alone reduced ERBB2 mRNA levels relative to AUF1 down-regulation, consistent with earlier described results (Fig. 1C).

Analogous to experiments measuring ERBB2 mRNA associated with cytosolic HuR immunoprecipitates (Fig. 2A), HDAC6 cytosolic immunoprecipitates were prepared in the presence or absence of SKBR3 exposure to HDACi (3 hours), and coprecipitating ERBB2 transcripts were measured by reverse transcription-PCR. Figure 3C indicates that SKBR3 cytosolic HDAC6 is enriched for ERBB2 3′ UTR mRNA, and this enrichment was not diminished even in the presence of LAQ824 (10 μmol/L ×3 hours). Unlike HDACi treatments which reduced ERBB2 mRNA and protein levels, siRNA induced HDAC6 knockdown sufficient to allow for α-tubulin acetylation resulted in slightly increased levels of SKBR3 ERBB2 protein after 72 hours (Fig. 3D). Consistent with these Western blots, Northern blots from the same cell treatments showed no significant change in ERBB2 mRNA levels (data not shown). These latter results indicate that HDAC6 protein knockdown is not functionally equivalent to catalytic inhibition of its deacetylase activity, and that α-tubulin acetylation does not functionally correlate with ERBB2 mRNA destabilization.

A series of novel HDAC6-selective inhibitors were synthesized to evaluate their effects on SKBR3 ERBB2 expression and growth. Figure 4A shows the structural differences between the hydroxamates ST17, ST80, and ST71 with *in vitro* assays demonstrating their 14-fold to 31-fold greater catalytic inhibition (IC_{50} values) of purified HDAC6 activity relative to HDAC1 activity, with ST80 showing the greatest selectivity (Table 1). The intracellular functionality of the HDAC6-selective inhibitors relative to the pan-HDAC inhibitor LAQ824 was determined by assaying the relative levels of the HDAC6-specific target, acetylated α-tubulin, to histone H4 acetylated at K12. As shown in Fig. 4B, SKBR3 cells treated with the HDAC6-selective inhibitors displayed significantly greater α-tubulin acetylation relative to histone H4 K12 acetylation when compared with the levels in LAQ824-treated cells, with ST80 displaying an 80-fold enhancement in the

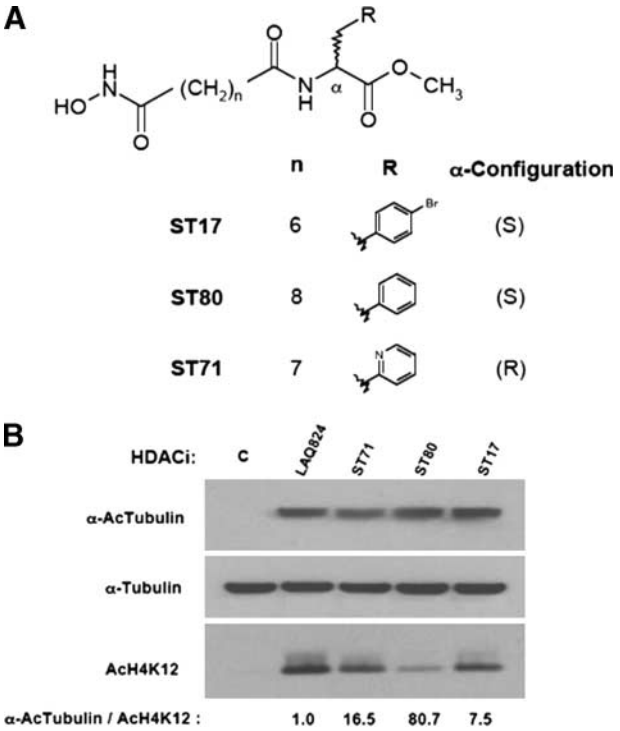

FIGURE 4. Structure and HDAC6-selective activity of three newly synthesized hydroxamic acids. **A.** Chemical structures of ST17, ST80, and ST71. **B.** Differential levels of acetylated α-tubulin (*α-AcTubulin*) and histone H4 K12 (*AcH4K12*) in whole cell lysates from SKBR3 cells treated for 24 h with 0.5 μmol/L of LAQ824 or 50 μmol/L of ST71, ST80, and ST17. Control (*c*) lysate from vehicle-treated SKBR3 cells. Densitometry determined ratios for α-AcTubulin/AcH4K12 were normalized by the values from LAQ824 treatment.

acetylated α-tubulin to acetylated K12 histone H4 ratio. The inability of any of these three HDAC6-selective hydroxamate inhibitors to repress endogenous *ERBB2* promoter activity after 24 hours of exposure to doses exceeding 50 μmol/L, as compared with the well described *ERBB2* promoter–repressing effects of submicromolar doses of other pan-HDAC–inhibiting hydroxamates (1-3), was shown using the same *ERBB2* promoter–reporting (luciferase expressing) MCF7/R06pGL-4 cell line formerly used to screen chemical libraries for cell-permeable drugs with specific *ERBB2* promoter–repressing functions (2). Figure 5A shows a representative dose-response comparison of ST71 with LAQ824 (after 24 hours of treatment) against MCF7/R06pGL-4 cells; although neither drug altered the viability of this ERBB2-independent subline (as measured by MTT assay) over this 24-hour treatment interval, the HDAC6-selective inhibitor was unable to repress luciferase expression at any drug dose in contrast to the pan-HDAC inhibitor which exhibited the expected dose-dependent repression of *ERBB2* promoter-driven luciferase activity. When ST71 and LAQ824 were compared for their ability to inhibit SKBR3 cell growth after 72 hours of continuous exposure, both showed dose-dependent antiproliferative activities, but LAQ824 exhibited 3-log greater potency (lower IC_{50}) over ST71 (Fig. 5B).

To confirm the effect of HDAC6-selective inhibitors on ERBB2 transcript decay, experiments were designed using SKBR3 cells pretransfected for 72 hours with HDAC6 siRNA. As shown in Fig. 6A, the HDAC6 siRNA–transfected SKBR3 cells were significantly less susceptible to LAQ824- or ST80-induced ERBB2 mRNA decay as control siRNA-treated cells. To assess the ability of antiproliferative doses of the HDAC6-selective inhibitors to promote ERBB2 protein down-regulation, Fig. 6B shows that following a 24-hour treatment of SKBR3 cells with 50 μmol/L of ST71, ST80, or ST17, suppression of ERBB2 protein levels were relatively equivalent to that achieved by 0.5 μmol/L of LAQ824.

Discussion

We initially reported that pan-HDAC inhibitors, although capable of repressing *ERBB2* promoter function and accelerating the decay of mature ERBB2 transcripts, are unable to affect ERBB2 mRNA expressed off an ectopic cDNA construct lacking both 5′ and 3′ *ERBB2* UTR sequences (1). By fusing the *ERBB2* 3′ UTR onto the terminus of a luciferase cDNA reporter and transfecting this into human breast cancer cells, we subsequently confirmed that the *ERBB2* 3′ UTR sequence is capable of accelerating transcript decay upon exposure (≥5 hours) to pan-HDAC inhibitors (7). Also, by using an expression array strategy to identify and quantitate all U-rich UTR-bearing genes endogenously expressed in SKBR3 cells, we showed that ERBB2 is among the more than 300 different U-rich transcripts (including cyclins D1 and D2, and the importin β family member exportin 4) which rapidly destabilized within 6 hours of treatment with such pan-HDAC–inhibiting hydroxamates such as TSA and LAQ824 (16). By sequence inspection of the conserved U-rich element (nucleotides 465-505; Fig. 1A) within the 3′ UTR of ERBB2, mRNA could putatively bind either the destabilizer, AUF1, or the stabilizer, HuR (5, 6). However, the present study shows that although both AUF1 and HuR are abundantly expressed in SKBR3 cells, only HuR seems capable of binding to the ERBB2 U-rich element (Fig. 1B) and regulating intracellular levels of ERBB2 mRNA and protein (Figs. 1C and 3B).

As cytosolic HuR immunoprecipitates were found to possess increased HDAC enzymatic activity (Fig. 2B), and numerous previous studies have shown that HDAC6 is the primary source of most cytoplasmic HDAC enzymatic activities (10-13), Western analysis of HuR immunoprecipitates confirmed the presence of HDAC6, and the reciprocal experiment confirmed the association of HuR with HDAC6 immunoprecipitates (Fig. 2C). This coassociation of HuR with HDAC6 was RNA-dependent; furthermore, confocal imaging in SKBR3 showed cytoplasmic and nuclear colocalization of HDAC6 with HuR (Fig. 2D). Similar to HuR, HDAC6 immunoprecipitates seemed to be enriched with ERBB2 transcripts, and this

Table 1. Selective *In vitro* Micromolar Activity (IC_{50}) of Inhibitors Against Deacetylase Activity of Affinity-Purified FLAG-tagged HDAC1 and HDAC6 Subtypes, Measured as Described in Materials and Methods

	HDAC1 (IC_{50})	HDAC5 (IC_{50})	Selectivity for HDAC6
ST17	22.86 ± 7.25	1.69 ± 0.91	13.5
ST80	28.61 ± 2.53	0.91 ± 0.44	31.4
ST71	82.60 ± 4.96	4.01 ± 1.61	20.6

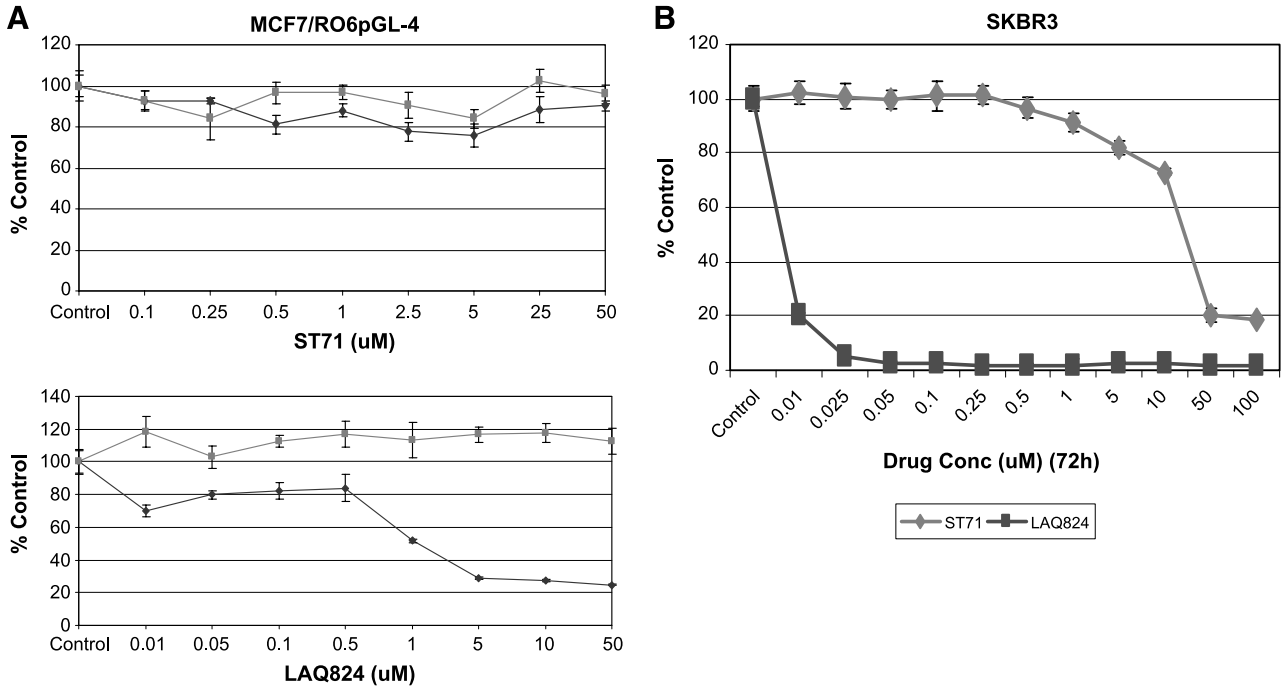

FIGURE 5. HDAC6-selective inhibitor ST71 fails to repress intracellular ERBB2 promoter activity but inhibits culture growth of ERBB2-positive SKBR3 cells. **A.** Dose-response comparison against *ERBB2* promoter-reporting (luciferase expressing) MCF7/R06pGL-4 cells following exposure to HDAC6-specific inhibitor ST71 or pan-HDAC inhibitor LAQ824, showing the effects of 24 h of treatment (% control) on endogenous luciferase expression (♦) and MTT cell viability (■). **B.** Dose-response comparison against ERBB2-positive SKBR3 cells after exposure to ST71 or LAQ824, with loss of MTT cell viability as a measure of growth inhibition following 72 h of treatment (% control).

association was maintained for at least 3 hours following treatment with an ERBB2 transcript destabilizing dose of HDACi (Fig. 3C). It remains unclear how HDAC6 physically associates with ERBB2 mRNA. Based on evidence provided here, it may be suggested that HDAC6, which has no structural means of directly binding to nucleic acids, associates with HuR in an RNA-dependent interaction (Fig. 2B); alternatively, HDAC6 may be tethered by an unknown RNA-binding protein to the 3′ UTR of ERBB2 transcripts.

HDAC6, although not essential for normal mammalian development (11, 12), has been shown to regulate cell shape and motility in human breast cancer cells (17), growth factor–induced endocytosis and nuclear receptor translocation in fibroblasts (11), and T cell–dependent antibody response (12) and chemotaxis in lymphocytes (14). Curiously, lymphocyte chemotaxis does not require the deacetylase activity but does require the protein scaffolding and BUZ functions of HDAC6 (14). In contrast, nuclear receptor translocation in fibroblasts is significantly more impaired by loss of HDAC6 catalytic function than by the total absence of HDAC6 protein (12). This complexity involving HDAC6 catalytic and noncatalytic functions likely explains the paradoxical observation that knockdown of SKBR3 HDAC6 protein levels by siRNA did not destabilize ERBB2 mRNA as did inhibition of HDAC6 catalytic activity by either selective or nonselective HDAC6 binding hydroxamates. ERBB2 transcript destabilization may require not only the absence of HDAC6 deacetylase activity but also the presence of HDAC6 protein to provide a scaffolding or shuttling function for the transport of destabilized mRNA from polyribosomes into decapping and degradation compartments, such as stress granules and the processing (P) body (5). In contrast to mRNA decay, ERBB2 protein decay is known to be mediated by cytoplasmic proteasome and aggresome systems (18), both of which can be inhibited by HDACi (13, 19). Thus, the modest increase in SKBR3 ERBB2 protein levels observed following siRNA knockdown of HDAC6 possibly reflects impairment in both these protein degradation systems induced by the HDAC6 knockdown. The availability of functionally active HDAC6-specific hydroxamates that either inhibit (e.g., tubacin) or fail to inhibit (e.g., niltubacin) its deacetylase activity might help to discern the relative importance of HDAC6 catalytic and noncatalytic functions in maintaining ERBB2 transcript stability. Also, further comparison of HDAC6 protein down-regulation by siRNA with HDAC6 enzymatic inhibition may delineate those cytoplasmic compartments involved in ERBB2 mRNA decay from those involved in ERBB2 protein degradation.

Tubacin was the first HDAC6-selective hydroxamate inhibitor identified, and was shown to bind and inhibit one of the two deacetylase domains in HDAC6 (20); it typically inhibits intracellular HDAC6 tubulin deacetylase activity at culture concentrations exceeding 10 μmol/L (14). The presently synthesized HDAC6-selective hydroxamate inhibitors ST17, ST80, and ST71 show comparable specificity relative to tubacin and modestly enhanced potency. They induce intracellular α-tubulin acetylation at drug concentrations ≥1 μmol/L; even after 24 hours of exposure to a 50 μmol/L concentration sufficient to induce almost complete growth arrest of SKBR3 cells,

these HDAC6-selective inhibitors predominantly induce α-tubulin acetylation relative to H4 acetylation (Fig. 4B). Similar to tubacin, these novel hydroxamates are useful chemical tools and prototypes for the development of more potent clinical drugs. As drug prototypes, these HDAC6-selective inhibitors show antiproliferative activity against SKBR3 cells at 3-log higher concentrations than that of one of the most potent pan-HDAC–inhibiting drugs to enter clinical development, LAQ824 (Fig. 5B). Following exposure to antiproliferative doses of these HDAC6-selective inhibitors, ERBB2 transcript and protein levels in SKBR3 cells declined just as rapidly as when these cells were treated with micromolar doses of LAQ824 (Fig. 6). The explicit involvement of HDAC6 in mediating ERBB2 mRNA decay was shown using SKBR3 cells pretransfected with siRNA that produced ~70% knockdown of HDAC6 protein levels (Fig. 3D); this partial HDAC6 knockdown was sufficient to reduce the ERBB2 mRNA destabilizing ability of both a pan-HDACi (LAQ824) and an HDAC6-selective (ST80) inhibitor (Fig. 6A).

Although LAQ824 and other previously evaluated pan-HDAC inhibitors repressed endogenous *ERBB2* promoter activity and accelerated the decay of mature ERBB2 transcripts (1), none of the HDAC6-selective inhibitors (ST17, ST80, and ST71) were able to affect endogenous *ERBB2* promoter function (Fig. 5A). These observations are consistent with the hypothesis that *ERBB2* promoter function is regulated by one or more class I nuclear HDACs (e.g., HDAC1, HDAC2, HDAC3, and/or HDAC8) whereas a major component of ERBB2 transcript stability seems to be regulated by the class II cytoplasmic deacetylase, HDAC6. Altogether, these findings point to the therapeutic potential of HDAC6-selective inhibitors, and serve to show that ERBB2 transcript stability mechanisms use targets such as HuR and HDAC6 that are readily exploitable for the design of new anticancer therapies. Future studies aimed at dissecting the ERBB2 transcript stability mechanism are clearly needed, as it seems particularly important to better understand the structural and functional interactions between HDAC6 and HuR, as well as their potential involvement with another 3′ UTR mRNA–associated stability mechanism, microRNA (21).

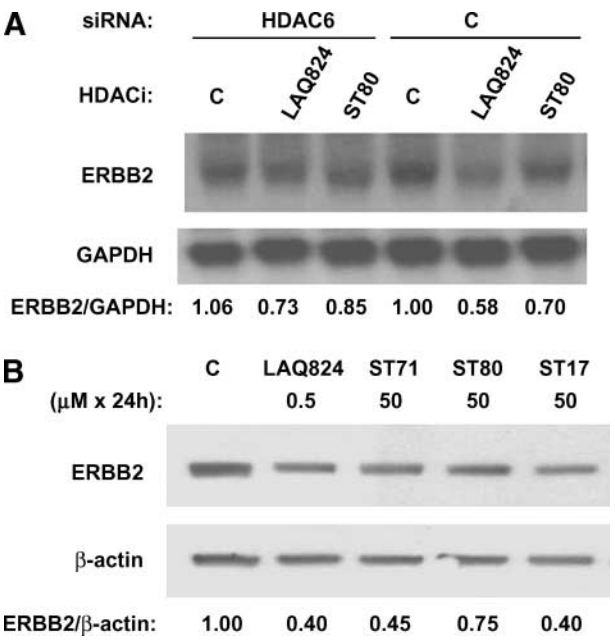

FIGURE 6. HDAC6 knockdown offsets ERBB2 mRNA decay induced by pan-HDACi and HDAC6-selective inhibitors that comparably reduce SKBR3 ERBB2 mRNA and protein levels. **A.** Northern blot showing the influence of 3 h of treatment with 0.5 μmol/L of LAQ824, 50 μmol/L of ST80, or vehicle control (*C*) on ERBB2 mRNA levels in SKBR3 cells pretransfected for 72 h with HDAC6 or control (*C*) siRNA. Densitometry determined ratios of ERBB2/GAPDH band intensities were normalized by the value obtained from vehicle-treated control siRNA transfectants (*C*). **B.** Western blots showing the effects of 24 h of treatment with the indicated drug and concentration on SKBR3 ERBB2 and β-actin protein levels; densitometry measured band intensities were used to calculate ERBB2/β-actin protein ratios, normalized such that untreated control (*C*) ratio = 1.

Materials and Methods

Cells, Culture Growth, and Luciferase Expression Assays

The human breast cancer cell line SKBR3 was originally obtained from the American Type Culture Collection and was grown in McCoys medium (Cellgro) supplemented with 10% fetal bovine serum and 1% penicillin/streptomycin. HCT116 human carcinoma cells were grown in DMEM (Mediatech) supplemented with 10% fetal bovine serum, 1% penicillin/streptomycin, and 2 mmol/L of L-glutamine (Life Technologies, Invitrogen). The luciferase-expressing ERBB2 promoter-reporting subline, MCF7/R067pGL-4, was constructed as previously described (1, 2) and was grown in DME H-16 medium supplemented with 10% fetal bovine serum, 10 μg/mL of insulin, 1% penicillin/streptomycin, and 500 μg/mL of neomycin (G418, Mediatech). Culture growth was measured using an MTT [3-(4,5-dimethylthiazol-2-yl)-2,5-diphenyltetrazolium bromide; Sigma-Aldrich] assay after plating cells into 96-well, 12-well, or 10 cm culture dishes, treating with drug or vehicle (0.5% DMSO) at the indicated concentrations and times. MTT was added to washed monolayers at a final concentration of 0.5 mg/mL (4 h), and absorbance of the colored soluble formazan product was quantitated at 570 nm by spectrophotometric microplate reader (Molecular Devices), as previously described (1, 2). Luciferase expression was measured from plated, treated, and washed cells after lysis (Passive Lysis Buffer E194A; Promega) using a commercial assay kit (Promega) and microplate luminometer (LabSystems Fluoroskan Ascent FL, Thermo Electron Corp.), as previously described (1, 2).

Hydroxamates and HDAC Assays

TSA was commercially obtained (Sigma-Aldrich) and LAQ824 was a kind gift from Novartis Pharmaceuticals, Inc.; these were prepared in 0.1 mol/L stock solutions kept in DMSO at −20°C and protected from light. Three new hydroxamates, ST17, ST80, and ST71 (Fig. 4), were synthesized by our previously established route using tritylhydroxylamine (for ST17) and benzylhydroxylamine (for ST80 and ST71) in the synthetic sequence (22). The identity and purity of each compound was confirmed by IR, nuclear magnetic resonance, and elemental analysis (data not shown). The relative HDAC-inhibiting potential of these compounds was first compared against an HDAC-enriched rat liver extract, as previously

described (23). The relative HDAC6-binding and -inhibitory specificity of the novel hydroxamates was tested using immunoprecipitated FLAG-tagged HDAC1 and HDAC6 subtypes (24, 25), and were scored as IC_{50} values calculated for each compound based on the inhibition of the enzymatic reactivity of a fluorescent small molecule substrate (26), as previously described (23). A commercially obtained fluorogenic deacetylation assay kit was also used to evaluate HDAC enzymatic activity in various cellular immunoprecipitates (Upstate). To confirm the intracellular specificity of the HDAC6-specific inhibitors, their ability to induce the acetylation of α-tubulin (α-AcTubulin), an HDAC6-specific substrate, relative to total acetylation of histone H4 (AcH4) or K12-acetylation of H4, substrates for nuclear-associated HDACs, was assessed by immunoblotting extracts from control and treated cells.

ERBB2 3′ UTR mRNA Binding Assays

The binding of intracellular HuR and AUF1 proteins to the ERBB2 3′ UTR U-rich mRNA element was measured by electrophoretic mobility shift assay, using an RNA probe spanning the conserved terminal U-rich mRNA element (nucleotides 465-505). Cytosolic extracts were incubated with 1 to 2 mg/mL of poly[d(I-C)] in 100 mmol/L of KCl, 10 mmol/L of Tris-HCl (pH 7.5), 2 mmol/L of DTT, and 20% vol/vol glycerol for 20 min at 23°C. The binding reaction was then initiated by adding a P^{32}-labeled RNA probe generated from a PCR fragment spanning the UTR U-rich region and incorporating a T3 RNA polymerase binding site for the production of sense strand transcripts, using P^{32} UTP as the labeled nucleotide in the T3 RNA polymerase reaction with the labeled RNA probe purified by Nuc Spin columns (Ambion). Some binding reactions were coincubated with antibodies to HuR (Santa Cruz Biotechnology) or AUF1 (Upstate). Following treatment of the RNA binding reaction with RNase T1 for 10 min at 23°C to eliminate unprotected RNA, the reaction products were electrophoretically separated on 4.2% acrylamide (29:1 acrylamide/bisacrylamide) gels in 0.5× Tris-borate EDTA [50 mmol/L Tris (pH 7.5), 50 mmol/L boric acid, and 1 mmol/L EDTA] running buffer at 150 V. Gels were vacuum-dried and gel-shifted bands were visualized by autoradiography.

Transient Transfection and siRNA Reagents

Validated siRNA reagents (and associated control siRNAs) specific for HuR and AUF1 (Qiagen) or HDAC6 (Dharmacon) were commercially obtained. Cells were transfected with the various siRNAs at a final concentration of 100 nmol/L using OligofectAMINE (Invitrogen) in serum-free medium for 7 h. Following transfection, cells were incubated for an additional 48 h (HuR, AUF1) or 72 h (HDAC6) in medium supplemented with 10% serum (± additional treatments as indicated), prior to RNA and/or protein extraction. Transfections were repeated thrice to assure the consistency of the results.

Immunoblotting and Immunoprecipitation

Cytosolic lysates used for immunoprecipitation were prepared from cells dounced in a hypotonic buffer containing 50 mmol/L of Hepes (pH 7.4), 10 mmol/L of KCL, 0.3% NP40, 10 mmol/L of $MgCl_2$, 100 units/mL of SUPERasein (Ambion), and mini-complete protease inhibitors (Roche Diagnostics). Following the removal of nuclei by centrifugation, the cytoplasmic lysate was brought to 50 mmol/L of KCl and incubated at 4°C for 5 h with either 0.2 μg of HuR, HDAC6, or control antibodies together with 12 μL of protein G Sepharose beads (GE Healthcare) per milliliter of lysate. The protein G beads from the immunoprecipitations were washed once at 4°C in wash buffer [20 mmol/L Tris (pH 7.4), 50 mmol/L KCL, 10 mmol/L $MgCl_2$, and 0.3% NP40], resuspended in 1× loading buffer [20 mmol/L Tris (pH 6.9), 2% SDS, 1% 2-mercaptoethanol, 50 mmol/L NaCl, and 10% glycerol], heated to 95°C for 10 min. Equal aliquots of immunoprecipitated material were electrophoresed using 4% to 12% gradient gels (Invitrogen), transferred to nitrocellulose (Amersham Bioscience) and probed for HuR and HDAC6 in hybridization buffers of 20 mmol/L Tris (pH 7.5), 130 mmol/L of NaCl, and 0.05% Tween 20 with 5% nonfat milk. Horseradish peroxidase–coupled goat anti-mouse (Bio-Rad) and native IgG horseradish peroxidase detection reagent (Pierce) were used for the detection of bound antibody by the manufacturer's chemiluminescence enhancement procedure. Western analysis of lysates prepared from whole cells solubilized in loading buffer using brief sonication was done as described above for immunoprecipitated samples. The antibodies used included ERBB2 (Calbiochem), β-actin (Abcam), α-tubulin (Sigma), acetylated α-tubulin (Sigma), AUF1 (Upstate), HuR (mouse 3A2; Santa Cruz Biotechnology), Lex A (mouse control antibodies for HuR immunoprecipitations; Santa Cruz Biotechnology), HDAC6 (sc-11420; Santa Cruz Biotechnology), ERα (rabbit control antibodies for HDAC6 immunoprecipitations; Santa Cruz Biotechnology) acetylated H4 (Upstate), or K12-acetylated H4 (Cell Signaling Technology).

Northern Blots and Reverse Transcription-PCR Detection of Specific Transcripts

RNA from control or treated cells was isolated using TRIzol (Invitrogen) according to the manufacturer's specifications. For Northern blotting, 15 μg of total RNA per lane was electrophoresed into 1% agarose-formaldehyde gels, then transferred onto Hybond Plus membranes (Amersham) that were UV cross-linked, hybridized with P^{32}-labeled cDNA probes for ERBB2 or GAPDH, and washed as previously described (1, 2). Hybridizing bands were visualized by autoradiography and quantified by densitometry (GS-710 Calibrated Imaging Densitometer; Bio-Rad), and transcript ratios (ERBB2/GAPDH) calculated. RNA isolated using TRIzol (Invitrogen) from cellular immunoprecipitates prepared as described above was reverse-transcribed by oligo-dT priming using SuperScript II reverse transcriptase (Invitrogen) in 20 μL volumes, according to the manufacturer's instructions, then subjected to PCR amplification using ERBB2-specific or GAPDH-specific primers (forward, reverse). GAPDH detection served as a control for nonspecific RNA binding to cellular immunoprecipitates. ERBB2-specific primers were designed to amplify a 137-nucleotide sequence within the ERBB2 3′ UTR, just upstream of the evolutionarily conserved terminal U-rich sequence (nucleotides 465-505). PCR reactions were done with Phusion (New England BioLabs) polymerase using 2 μL

aliquots from the reverse transcription reactions with primers at 1 μmol/L final concentration. The linearity of the PCR reactions were confirmed by examination of identically prepared reactions following 23 to 26 cycles. Reaction products were examined on precast 8% polyacrylamide Tris-borate EDTA gels (Invitrogen) using HaeIII cut PhiX DNA markers (New England BioLabs) and visualized by ethidium bromide staining. Primer pairs used were as follows:

ERBB2 (137 bp amplimer)
forward: 5′ GGTACTGAAAGCCTTAGGGAAGC 3′
reverse: 5′ ACACCATTGCTGTTCCTTCCTC 3′
GAPDH (234 bp amplimer)
forward: 5′ CGAATTGGCTACAGCAACAGG 3′
reverse: 5′ GTACATGACAAGGTGCGGCTC 3′

Immunofluorescence Imaging

SKBr3 cells were fixed and incubated with rabbit polyclonal anti-HDAC6 and mouse monoclonal anti-HuR primary antibodies (Santa Cruz Biotechnology), followed by donkey anti-rabbit Alexa 555 and anti-mouse Alexa 488 secondary antibodies (Invitrogen). Cells were visualized using an LSM 510 NLO Confocal Scanning System (mounted on an Axiovert 200 Inverted Microscope; Carl Zeiss Ltd.) equipped with a two-photon Chameleon laser (Coherent, Inc.). Confocal images were generated using a 40× objective with 4× digital zoom, processed by Imaris software including analysis by the colocalization module (Bitplane AG).

Disclosure of Potential Conflicts of Interest

No potential conflicts of interest were disclosed.

Acknowledgments

LAQ824 was generously provided by Novartis Pharmaceuticals, Inc. (East Hanover, NJ).

References

1. Scott GK, Marden C, Xu F, Kirk L, Benz CC. Transcriptional repression of ErbB2 by histone deacetylase inhibitors detected by a genomically integrated ErbB2 promoter-reporting cell screen. Mol Cancer Ther 2002;1:385–92.

2. Marx C, Berger C, Xu F, et al. Validated high-throughput screening of drug-like small molecules for inhibitors of ErbB2 transcription. Assay Drug Dev Technol 2006;4:273–84.

3. Drummond DC, Noble CO, Kirpotin DB, Guo Z, Scott GK, Benz CC. Clinical development of histone deacetylase inhibitors as anticancer agents. Annu Rev Pharmacol Toxicol 2005;45:495–528.

4. Drummond DC, Marx C, Guo Z, et al. Enhanced pharmacodynamic and antitumor properties of a histone deacetylase inhibitor encapsulated in liposomes or ErbB2-targeted immunoliposomes. Clin Cancer Res 2005;11:3392–401.

5. Barreau C, Paillard L, Osborne B. AU-rich elements and associated factors: are there unifying principles? Nucleic Acids Res 2005;33:7138–50.

6. Lopez de Silanes I, Zhan M, Lal A, Yang X, Gorospe M. Identification of a target RNA motif for RNA-binding protein HuR. Proc Natl Acad Sci U S A 2004;101:2987–92.

7. Marx C, Berger C, Benz S, Mattie M, Benz C, Scott G. Therapeutic destabilization of ErbB2 transcripts mediated by U-rich mRNA binding proteins and microRNAs. Proc Am Assoc Cancer Res 2006;47:a5616.

8. Heinonen M, Bono P, Narko K, et al. Cytoplasmic HuR expression is a prognostic factor in invasive ductal breast carcinoma. Cancer Res 2005;65:2157–61.

9. Wang W, Yang X, Kawai T, et al. AMP-activated protein kinase-regulated phosphorylation and acetylation of importin α1. J Biol Chem 2004;279:48376–88.

10. Hubbert C, Guardiola A, Shao R, et al. HDAC6 is a microtubule-associated deacetylase. Nature 2002;417:455–8.

11. Gao Y, Hubbert CC, Lu J, Lee Y-S, Lee J-Y, Yau T-P. Histone deacetylase 6 regulates growth factor-induced actin remodeling and endocytosis. Mol Cell Biol 2007;27:8637–47.

12. Zhang Y, Kwon S, Yamaguchi T, et al. Mice lacking histone deacetylase 6 have hyperacetylated tubulin but are viable and develop normally. Mol Cell Biol 2008;28:1688–701.

13. Matthias P, Yoshida M, Khochbin S. HDAC6, a new cellular stress surveillance factor. Cell Cycle 2008;7:7–10.

14. Cabrero JR, Serrador JM, Barreiro O, et al. Lymphocyte chemotaxis is regulated by histone deacetylase 6 independently of its deacetylase activity. Mol Biol Cell 2006;17:3435–45.

15. Zhang Z, Yamashita H, Toyama T, et al. HDAC6 expression is correlated with better survival in breast cancer. Clin Cancer Res 2004;10:6962–8.

16. Benz SC, Scott GK, Marx C, Melov S, Benz CC. Histone deacetylase inhibitors accelerate decay of unique subsets of breast cancer transcripts that include ErbB2. Proc Am Assoc Cancer Res 2005;46:a5.

17. Saji S, Kawakami M, Hayashi S, et al. Significance of HDAC6 regulation via estrogen signaling for cell motility and prognosis in estrogen receptor-positive breast cancer. Oncogene 2005;24:4531–9.

18. Marx C, Yau C, Banwait S, et al. Proteasome-regulated ERBB2 and estrogen receptor pathways in breast cancer. Mol Pharmacol 2007;71:1525–34.

19. Place RF, Noonan EJ, Giardina C. HDAC inhibition prevents NF-κB activation by suppressing proteasome activity: down-regulation of proteasome subunit expression stabilizes IκBα. Biochem Pharmacol 2005;70:394–406.

20. Haggarty SJ, Koeller KM, Wong JC, Grozinger CM, Schreiber SL. Domain-selective small-molecule inhibitor of histone deacetylase 6 (HDAC6)-mediated tubulin deacetylation. Proc Natl Acad Sci U S A 2003;100:4389–94.

21. Scott GK, Goga A, Bhaumik D, Berger CE, Sullivan CS, Benz CC. Coordinate suppression of *ERBB2* and *ERBB3* by enforced expression of microRNA *miR-125a* or *miR-125b*. J Biol Chem 2007;282:1479–86.

22. Jung M, Hoffmann K, Brosch G, Loidl P. Analogues of trichostatin A, trapoxin B as histone deacetylase inhibitors. Bioorg Med Chem Lett 1997;7:1655–8.

23. Heltweg B, Jung M. A homogeneous non-isotopic assay for histone deacetylase activity. J Biomol Screen 2003;8:89–95.

24. Fischle W, Emiliani S, Hendzel MJ, et al. A new family of human histone deacetylases related to *Saccharomyces cerevisiae* HDA1p. J Biol Chem 1999;274:11713–20.

25. Fischle W, Dequiedt F, Hendzel MJ, et al. Enzymatic activity associated with class II HDACs is dependent on a multiprotein complex containing HDAC3 and SMRT/N-CoR. Mol Cell 2002;9:45–57.

26. Heltweg B, Dequiedt F, Verdin E, Jung M. A non isotopic substrate for assaying both human zinc and NAD^+-dependent histone deacetylases. Anal Biochem 2003;319:42–8.

Molecular Cancer Research

Destabilization of ERBB2 Transcripts by Targeting 3′ Untranslated Region Messenger RNA Associated HuR and Histone Deacetylase-6

Gary K. Scott, Corina Marx, Crystal E. Berger, et al.

Mol Cancer Res 2008;6:1250-1258.